Numerical Study on the Flow Characteristics of 2-D Free Jet at a Low Reynolds Number

IOP Conf. Series: Materials Science and Engineering **491** (2019) 012025 doi:10.1088/1757-899X/491/1/012025

Numerical Study on the Flow Characteristics of 2-D Free Jet at a Low Reynolds Number

B Shin[1,*] **and S Tashiro**[2]

[1] Department of Mechanical Design Systems Engineering, University of Miyazaki, Miyazaki 889-2192, Japan
[2] Graduate School of Engineering, University of Miyazaki, Miyazaki 889-2192, Japan

[*] Corresponding Author: brshin@cc.miyazaki-u.ac.jp

Abstract. Two-dimensional free jets have been numerically studied in the laminar flow regime. The numerical solution was obtained by solving the incompressible Navier-Stokes equations with SMAC finite-difference method. The variation of the axial velocity, potential core and jet spreading width were investigated to make clear the characteristics of free jet at a low Reynolds number. It was found that the fully developed region where the self-similarity is satisfied exists in the downstream of the collapsing point of the potential core. The variation of the core is depended on the Reynolds number. It showed that the half-width of geometry is useful in identifying the similarity. The predicted velocity distributions were in good agreement with those of experimental and theoretical results.

1. Introduction

Jet flow is one of the fundamental and important topics in fluid mechanics, and due to its geometric simplicity it has been studied in various fields such as fluids and combustion engineering, and can be seen in a variety of fields around us. In the jet flow, the boundary of the jet, spread, flow distance, shear structure, and heat transfer effects are sensitive to the structure of the initial stages of the jet. Especially in this regime, the intermixing of complex flow elements such as instability, coherent structure, and entrainment flow due to the development of free shear flow exist, therefore it is difficult to analyze. Many theoretical and experimental researches on free jet have been studied up to now since free jet flow is known to have a self-preservation and similarity [1]-[5]. In particular, theoretical analysis on the characteristics of laminar jet by Schlichting [1] has been well known but is based on boundary layer theory, and thus the velocity distribution at the outer edge of the jet flow do not match those from experimental results even in regimes where similarity laws are valid. In order to solve this problem, various theoretical studies have been conducted for decades [6]-[11]. Unfortunately, however, almost of them introduce the concept of boundary layer, there is naturally a limit to which it could be applied to various flow regions including the initial region of the jet flow. On the other hand, in recent years, due to the improvement in computational environment and rapid propagation of computational fluid dynamics (CFD), numerical analysis of complex flow phenomenon has been conducted. Research done with CFD is advantageous when analyzing jet flow accompanying the flow phenomena change due to flow conditions such as Reynolds number or the shape of the nozzle, but are mostly focused on turbulent flow at the high Reynolds number, and very few studies focus on the low Reynolds number regime.

In this study, a computational code based on SMAC finite difference method [12] was developed in order to investigate the jet flow characteristics at the low Reynolds number (*Re*) regimes from the initial jet flow region to the fully developed region, and the two-dimensional (2-D) incompressible free jet in the range of *Re* = 30 - 300 is numerically analyzed. Also, from the analysis, characteristics of free jet such as variation of the axial velocity, similarity, potential core and jet spread of the jet flow are clarified.

2. Numerical method

2.1. Fundamental equations and SMAC scheme

The fundamental equations for the numerical simulation are the continuity equation and the incompressible Navier-Stokes equations.

$$\nabla \cdot \boldsymbol{u} = 0 \tag{1}$$

$$\frac{\partial \boldsymbol{u}}{\Delta t} + \nabla \cdot \boldsymbol{u}\boldsymbol{u} = -\nabla p + \frac{1}{Re}\nabla^2 \boldsymbol{u} \tag{2}$$

In this study, the fundamental equations (1) and (2) can be written by applying the Simplified MAC (SMAC) scheme as [13]

$$\frac{\boldsymbol{u}^* - \boldsymbol{u}^n}{\Delta t} = -\nabla p^n + (\frac{1}{Re}\nabla^2 \boldsymbol{u} - \nabla \cdot \boldsymbol{u}\boldsymbol{u})^n \tag{3}$$

$$\frac{\boldsymbol{u}^{n+1} - \boldsymbol{u}^*}{\Delta t} = -\nabla \phi \tag{4}$$

$$\nabla^2 \phi = \frac{\nabla \cdot \boldsymbol{u}^*}{\Delta t} \tag{5}$$

$$p^{n+1} - p^n = \phi \tag{6}$$

where $\boldsymbol{u}$, and p denote the velocity and pressure, and ϕ represents the pressure increments, superscript n is the time level, asterisk * denotes the intermediate time level between n and n+1. In the computation of SMAC scheme, the dependent variables $\boldsymbol{u}$ and p are defined at different points of the staggered grid. The use of such a staggered grid is advantageous in that spurious errors are completely removed as in the MAC scheme. The Euler forward scheme was used to discretize the time derivative term, and for the spatial derivative, the 2nd order central difference method was basically applied. However, in the computation of high Reynolds numbers flow, a QUICK scheme [14] in the convection term was used in order to obtain accuracy and stability of the computation. Also, the boundary value problems in equation (5) were determined by using the SOR method with a maximum iteration number of 20.

2.2. Computational domain and boundary conditions

As can be seen from figure 1, the computational domain was set by 100*d* in the *x* direction, $\pm$30*d* in the *y* direction from the center of the nozzle with 2000×1200 square grids, where *d* represents the nozzle width. The boundary conditions were imposed by the initial velocity distribution at the nozzle exit, the Dirichlet conditions for pressure at the downstream, and the Neumann conditions for velocity and pressure in all other regions. Also, the Reynolds number was defined by the average velocity at the nozzle exit and the nozzle width *d*.

3. Numerical results

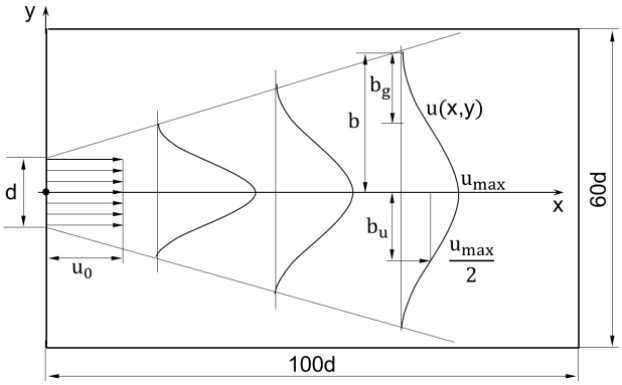

Figure 1. Jet flow geometry and computational domain.

3.1. Comparison with experimental and theoretical results

First, in order to check the accuracy and reliability of the present jet flow code by the SMAC scheme, predicted results were compared with exiting results. In this computation, iterative computations of the explicit time-marching method with Δt of 0.02 were conducted. The converged solution was obtained when the continuity conditions were lower than 1×10^{-5}. The time average values were taken from the solutions for 200 non-dimensional times.

Figure 2 shows time averaged axial velocity distributions at several downstream sections with non-dimensional distance y/d, when the velocity distribution (u_0) of the Poiseuille flow with Re = 457 is set as the initial condition at the nozzle exit for comparison with experiments. In this Reynolds number regime, the jet flow basically showed an asymmetric unsteady flow behaviour [15], but the time averaged velocities are in good agreement with experimental results [2] from the initial region of the jet to the fully developed regions, for instance, at x/d = 3 and 10.

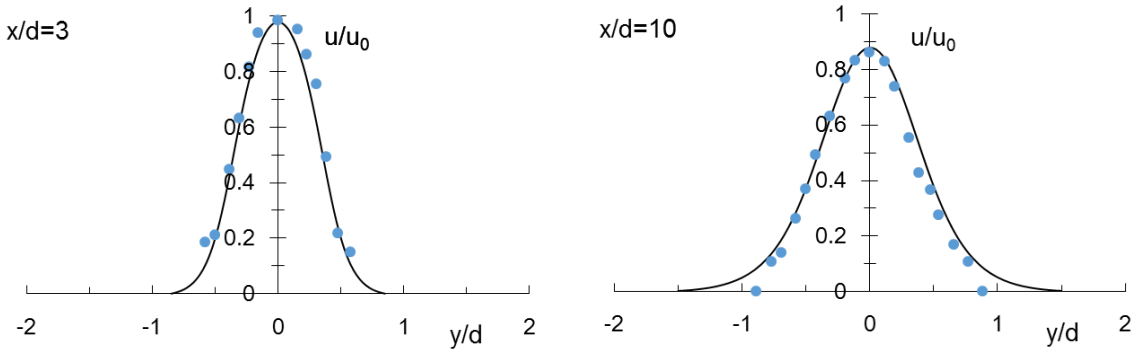

Figure 2. Velocity distribution of Poiseuille flow jet in two different sections of x/d at Re = 457.

Figure 3 shows the axial direction velocity distribution at Re = 200 with the uniform flow boundary condition at the nozzle exit. Here, axial velocity u is normalized by the maximum velocity u_{max} on the centre line at given x/d. In general the numerical results well predicted compared with the experimental results [7] as in the case of Poiseuille flow conditions, especially at regions extremely close to the nozzle exit. Figure 4 depicts a comparison of the present prediction to Schlichting's theoretical solutions [1]. These results were obtained from the computations with the initial conditions

of the Poiseuille flow and the uniform flow at the nozzle exit. In this figure, y is normalized by the half width of velocity $b_u$which is the distance from the centre line to the point where u/u_{max}=0.5. At fully developed flow regions (for example x/d = 15), the present predictions are in good agreement to the theoretical solutions even if the inflow conditions are different from each other. There is a somewhat discrepancy near the outer edge, but it is due to the fact that at theoretical solutions based on the theory of boundary layer: the solution is determined by $u = 0$ at $y \rightarrow \infty$. As investigated so far, the present method well simulated the 2-D jet flow velocity filed from the nozzle exit to the fully developed region where the self-similarity is satisfied with high accuracy, resulting that the present numerical method is considered to be sufficiently reliable.

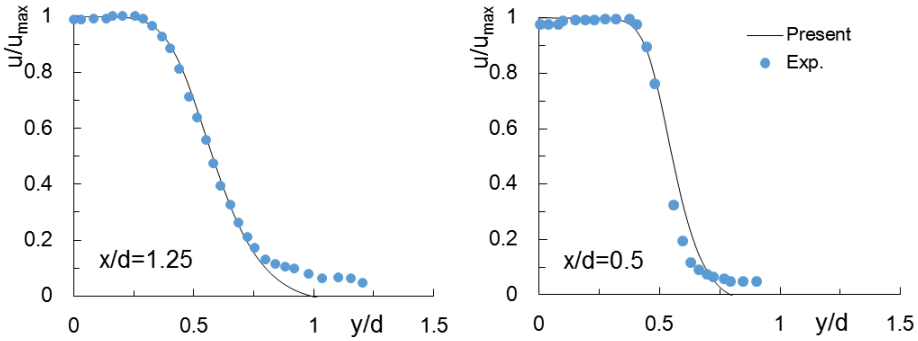

Figure 3. Velocity distribution of uniform flow jet in two different sections near the nozzle exit at *Re* = 200.

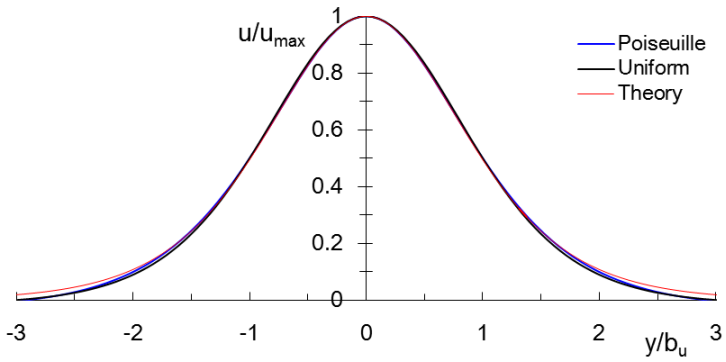

Figure 4. Velocity distribution of Poiseuille flow jet and uniform flow jet in the section of x/d = 15 at *Re* = 100.

3.2. Characteristics of velocity distribution

In order to investigate the jet velocity at an arbitrary cross section in the axial direction, figure 5 shows the axial velocity profiles along the y/b_u from the initial region to the developing region. This result was obtained from the uniform flow boundary condition with *Re* of 100. At initial regions close to the nozzle, the distribution is far from a Gaussian curve, shows large deviation from the similarity laws of velocity, but as the flow reaches downstream the jet flow develops, and approximately at regions after $x > 6d$, the similarity in velocity profiles begin to appear. Also, since these profiles are in good agreement with Sato and Sakao's experimental results [15] as well as with the analytical solution by Schlichting [1], it could be known that these distributions, just as results in figure 4, are nearly velocity profiles at fully developed flow regions which satisfy the self-similarity of jet.

On the other hand, there are several ways to estimate the characteristics of the jet depending on the choice of non-dimensional parameters [16]. Figure 6 indicates axial velocity profiles with respect to non-dimensional distance by half width of geometry b_g(=b/2, see figure 1) instead of b_u. As in figure 5, it could be seen that the jet will develop toward the downstream and the velocities satisfy the

similarity in the fully developed regions. In figure 5, however, velocity curves by the half width of velocity are difficult to distinguish among them since the curves have two fixed points at y/b_u of 0.0 and 1.0, but for ones with half width of geometry in figure 6, the differences in velocity distribution in the developing and developed regions are easy to know. Therefore, the evaluation of velocity distribution using the half width of geometry is useful for observing jet flow development.

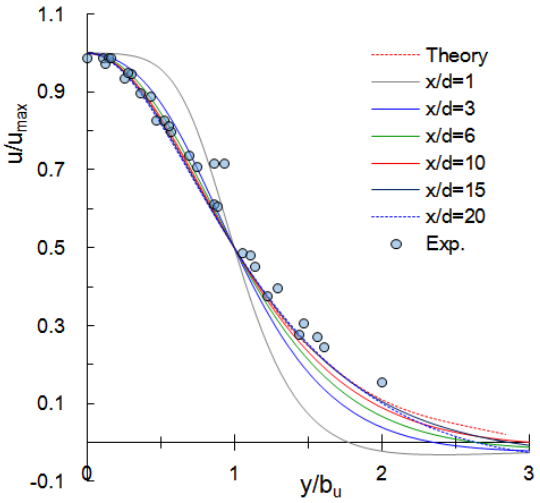

Figure 5. Axial velocity profiles with respect to the half-width of velocity in several downstream sections of *x*/*d* at *Re* = 100.

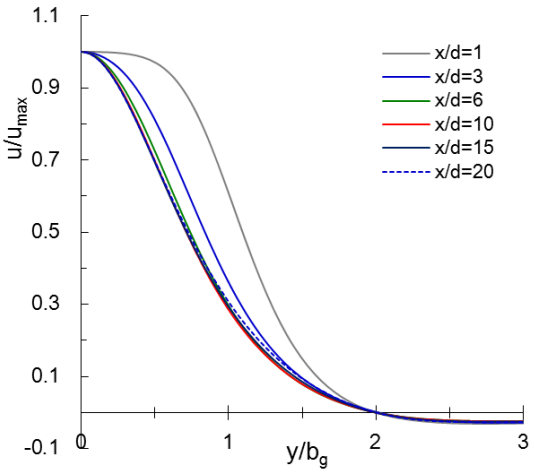

Figure 6. Axial velocity profiles with respect to the half-width of geometry in several downstream sections of *x*/*d* at *Re* = 100.

Figure 7 shows the change in velocity distribution with respect to non-dimensional distance [6] using half width of velocity and distance (x) in the axial direction. The variation of velocity due to this non-dimensional parameter shows the distinction of boundary between initial regions and regions satisfying similarity more vividly compared to figures 5 and 6. Figure 8 depicts the variation of velocity with respect to the non-dimensional parameter $(y - b_g)/x$, which uses the half width of geometry to imitate figure 7. As discussed in figure 6, the evaluation using the half width of geometry shows the transition of the velocity change clearer than that of the half width of velocity, and even at developed regions with $x/d \geq 6$, shows less overlap than compared to figures 6 and 7. From this, it could be inferred that at *Re* = 100, the fully developed region which satisfy similarity locates on the downstream after following transient process after breakdown of the potential core (refer to figure 9).

3.3. Potential core

Figure 9 plots the distance to the position where the potential core collapses. Here, the potential core length, x_p, was defined as the distance from the nozzle exit to the point where $u_c \approx 0.95u_0$. u_c and u_0 represent axial velocities at the jet centre and the nozzle exit, respectively. When $Re \leq 300$, x_p extends toward downstream with almost linear gradient of $x_p/d \approx 0.04Re$, but as a result of additional investigation for regions of $Re > 300$, the gradient was decreased to around $14 \leq x_p/d \leq 15$. These results are somewhat different from the case of turbulence flow known as $x_p/d = 12$ [17]. Figure 10 illustrates the change in the width of potential core (y_p/y_0) along the dimensionless distance $\xi(= (x/d)/Re)$ in the axial direction [8],[18] with the half width of nozzle y_0. It could be seen that the core region decreases and eventually disappears as x moves downstream from the nozzle exit. In the

range of $100 \leq Re \leq 300$, the relationship between change in y_p/y_0 and ξ is in approximately similarity, and as seen in figure 9, the distance when the potential core breaks down is around ξ = 0.04.

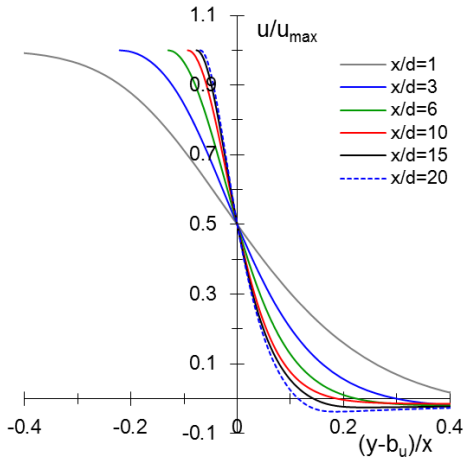

Figure 7. Axial velocity profiles with respect to the $(y - b_u)/x$ in several downstream sections of *x*/*d* at *Re*=100.

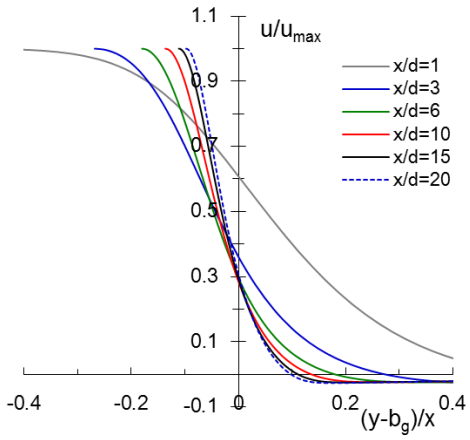

Figure 8. Axial velocity profiles with respect to the $(y - b_g)/x$ in several downstream sections of *x*/*d* at *Re*=100.

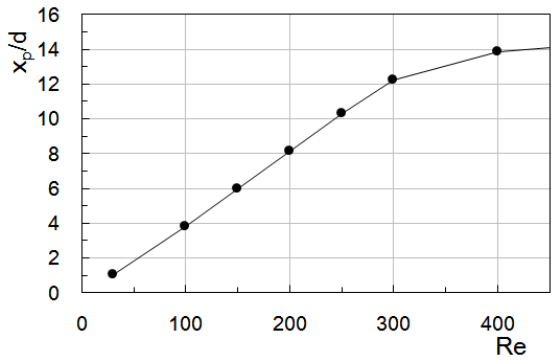

Figure 9. Potential core length with Reynolds number.

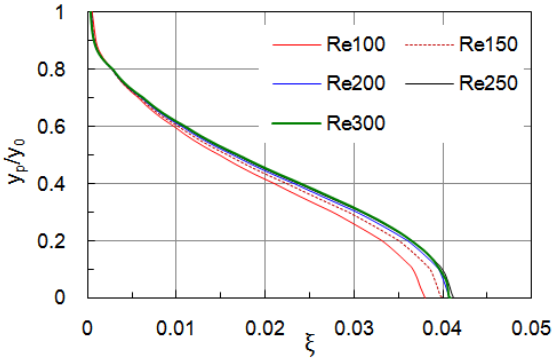

Figure 10. Variation of potential core width with $(x/d)/Re$.

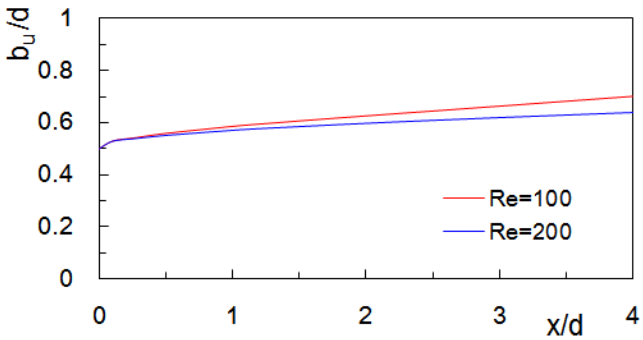

Figure 11. Variation of jet spread with half-width of velocity along the jet axis at Reynolds numbers of 100 and 200.

3.4. Jet spread

Figure 11 depicts the variation of jet spread. Jet spread is one of the most important fundamental characteristics in the analysis of jet flow characteristics. In this study, therefore, the jet width and its change over the axial direction were investigated by using the half width of velocity. The jet width spreads as the flow flows downstream from the nozzle exit, and in contrast to figure 10, as the Reynolds number increases the spread gradient tends to decrease. Also, it is confirmed that the tendency of jet spread obtained from this simulation is almost same as the experimental investigation [7].

4. Conclusions

In order to investigate the jet flow characteristics at the low Reynolds number regimes, two-dimensional incompressible free jets were computed by using SMAC finite difference method. By comparing the numerical results with experimental and theoretical results, it was confirmed that the present numerical method is sufficiently reliable to predict the jet flow with accuracy. From the investigation of the axial velocity distribution, similarity, potential core and jet spread of free jet, it was clarified the 2-D jet flow characteristics in the wide range of jet from the initial jet flow region to the fully developed region, which was difficult with the conventional analytical method. Also, it showed that the evaluation of velocity distribution by the half width of geometry is useful for observing jet flow development.

Acknowledgments

This work was partly supported by JSPS KAKENHI Grant Number JP17K06164.

References

[1] Schlichting H 1979 *Boundary Layer Theory* (New York: McGraw-Hill)
[2] Eugene P S and Thomas L L 1971 *Experimental Investigation of an Axisymmetric Fully Developed Laminar Free Jet* (NASA TN D-6304)
[3] Thomas L L and Eugene P S 1972 *Experimental Investigation of an Axisymmetric Free Jet with an Initially Uniform Velocity Profile* (NASA TN D-6783)
[4] Deo R C, Mi J and Nathan G J 2008 *Phys. Fluids* **20-**075108 p 075108-01
[5] Grandchamp X, Fujiso Y, Wu B and Hirtum A Van 2012 Steady *ASME J. Fluids Eng.* **134** p 011203
[6] Wygnanski I and Fiedler H 1969 *J. Fluid Mech.* **38** pp 577-612
[7] Greene G C 1974 *Comparison of measured and calculated velocity profiles of a laminar incompressible free jet at low Reynolds numbers* (NASA TN D-7510)
[8] Hatta K and Nozaki T 1975 Two-Dimensional and Axisymmetric Jet Flows with Finite Initial Cross Sections *Bulletin JSME* **18** pp 349-357
[9] Akaike S and Nemoto M 1988 *ASME J. Fluids Eng*. **110** pp 392-398
[10] Lee D D, Kihm K D and Chung S H 1997 *ASME J. Fluids Eng.* **119** pp 716-718
[11] Pani B S, Lee Joseph H W and Lai Adrian C H 2009 *J. Hydro-environment Research* **3** pp 121-128
[12] Amsden A A and Hallow F H 1970 *J. Comput. Phys.* **6** pp 322-325
[13] Shin B R and Ikohagi T 1991 *Computers & Fluids* **19** pp 479-488
[14] Leonard B P 1979 *Computer Methods in Appl. Mech. and Eng*. **19** pp 59-98
[15] Sato H and Sakao F 1964 *J. Fluid Mech.* **20** pp 337-352
[16] Abramovich G N 1963 *The Theory of Turbulent Jets* (Cambridge: MIT Press)
[17] Rajaratnam N 1976 *Turbulent Jets* (Amsterdam: Elsevier Sci. Pub. Co)
[18] Rankin G W, Sridhar K, Arulraja M and Kumar K R 1983 *J. Fluid Mech.* **133** pp 217-231